2012

Fabrication of Anisotropic Sol-gel Materials by Photo-Crosslinking

Charles Wingfield
Virginia Commonwealth University

Fabrication of Anisotropic Sol-gel Materials by Photo-Crosslinking

A thesis submitted in partial fulfillment of the requirements for the degree of Master of Science in Physics / Applied Physics at Virginia Commonwealth University.

By

Charles C. Wingfield

B.S. in Physics

Virginia Commonwealth University, 2010

M.S. in Physics/Applied Physics

Virginia Commonwealth University, 2012

Director:

Massimo F. Bertino

Associate Professor, Department of Physics

Virginia Commonwealth University,

Richmond, Virginia, 23284

5-05-2012

Acknowledgements

Fluff goes here

Table of Contents

Fabrication of Functionally Graded and Cellular Aerogels

By Chuck Wingfield

A thesis submitted in partial fulfillment of the requirements of the degree of

Master of Science at Virginia Commonwealth University.

Virginia Commonwealth University, 2012.

Major Director:

Dr. Massimo F. Bertino

Associate Professor, VCU Department of Physics

This is a report on the fabrication and characterization of anisotropic, porous materials: functionally graded cellular and compositionally anisotropic aerogels. This new class of materials was fabricated by photopolymerization of selected regions of a homogeneous monolith using visible light. Visible light is not significantly absorbed and not significantly scattered by organic molecules and oxide nanoparticles in wet gels and it allows fabrication of deeply penetrating, well-resolved patterns. Simple variations of the exposure geometry allowed fabrication of a wide variety of anisotropic materials without requiring layers or bonding.

Chapter 1: Silica Aerogel Reinforcement

1.1 Motivation

Silica aerogel was first produced by Samuel Kistler in 1931 on a bet with Charles Learned about who could replace the liquid in a jelly with gas without causing shrinkage. And on that, silica aerogel was born. Silica aerogel is an extremely porous silicon dioxide material which, because of its high surface area and extremely low density, is a very promising material for a list of applications. These properties include a very low thermal conductivity (0.01 W /(m·K)), relative chemical inertness, an extremely low density (0.01 g/cm^3), a surface area as high as 1200 m^2/g, it can withstand temperatures lower than 950°C without deformation for long periods of time and temperatures approaching 1200°C for short intervals, has a refractive index as low as 1.01, and can be made almost optically clear.[1-4] Additionally, using a suitable olefin, one can modify the surface of the pore wall and derivatize the walls to allow for a desired reaction setting.[5]

However, even with all of these remarkable properties, aerogels have only been used for high-end and niche applications due to a few major drawbacks. First, and most importantly, aerogels are extremely mechanically weak.[5] This is due in large part to the fact that aerogel is roughly composed of 95% air and 5% silica. The glass sponge nature should not come as a surprise to anyone, however for it to be handled easily, improvements have to be made. The second drawback of aerogels is that they must be

supercritically dried to remove the solvent. Supercritical drying requires you to take a fluid/gas beyond its supercritical point which can be very slow as well as costly. For example, ethanol requires a temperature of at least 270° C and pressure in excess of 1000 psi. Because of these factors, the handling and manufacturing costs of making monolithic aerogels make it very difficult to scale up and are large contributing factors to the niche applicability of aerogel.[4]

Some progress has been made over the past decade to resolve both issues.[4] This work will only concern itself with the problem of mechanical weakness, which appears to be a more limiting factor for the industrial development of silica aerogel. Several groups have made attempts to rectify this problem and their approaches will be explained in the next section.[4-10]

1.2 Literature Review

Several approaches have been taken to help improve the mechanical properties of aerogels. Layering sols of different densities has been attempted with some success, but due to the time consumptive nature, is not yet feasible. Cross-linking the oxides and adding structural support via a polymer backbone has also been attempted.[4] Polymer reinforcement was our primary area of focus because of the versatility of the technique as well as some unresolved issues left by previous works.[5]

In 2004, *Leventis et al.* published a communication in *Chemistry of Materials* where they reported about polymer reinforcement in surface-modified silica aerogels. In this communication, a polymer (polyurea) was used to structurally reinforce the sol-gel.

This polymer was only used as shown in Figure 1.1. *Leventis et al.* used an amine functional group that leaves a dangling olefin on the surface of the silica gel wall (as explained more in 2.1: Synthesis) which would give a bonding site for an active monomer, in this case, hexamethylene diisocyanate oligomer (Figure 1.2). This bonding site allows for the polymer to conformally coat the silica aerogel surface and be anchored chemically as shown in the SEM images in Figure 1.3.

In their communication, *Leventis et al.* claim a modulus of elasticity increase of a factor of 100 times over native silica aerogel due to the polymer reinforcement as shown in Figure 1.4. However, these gains came at the expense of an increased density and decreased surface area. Native aerogels had a density of 0.189 g/cm^3 as compared to the amine-modified, cross-linked aerogels which had a density of 0.439 g/cm^3. Correspondingly the surface area for a native gel was 997 m^2/g and for an amine-modified, cross-linked aerogel the surface area was 178 m^2/g.

So while *Leventis et al.* were able to get sizeable mechanical strength gains, the additional polymer took up space in the pores of the aerogel which adversely affected the porosity and the density. The thermal conductivity also increased from 0.01 W /(m·K) to 0.04 W /(m·K). This increase of a factor of 4 is very significant because, for reference, Styrofoam has a thermal conductivity as low as 0.03 W /(m·K) while having a density very comparable to some of the least dense isotropically reinforced aerogels. This means that isotropic reinforcement of aerogels will at best yield materials very similar in nature to Styrofoam, but with significantly increased costs and processing times.

Since *Leventis et al.* released their original publication in 2002, many different types and combinations of polymers, synthesis techniques, and conditions have been used to improve the mechanical properties of the aerogel, but unfortunately, very few results have shown any significant progress in altering the mechanical properties without adversely affecting the thermal conductivity or porosity of the aerogel.[4]

Chapter 1 Figures

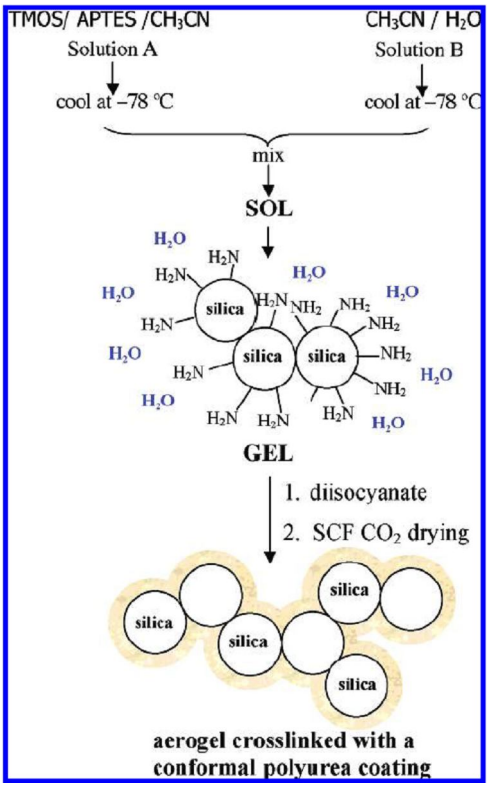

Figure 1.1
Structural reinforcement of Silica Aerogels via surface modification and polymer crosslinking

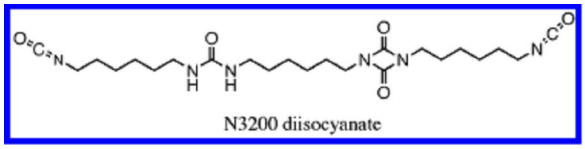

Figure 1.2
poly(hexamethylene diisocyanate) which was used as a cross-linker by *Leventis et al*

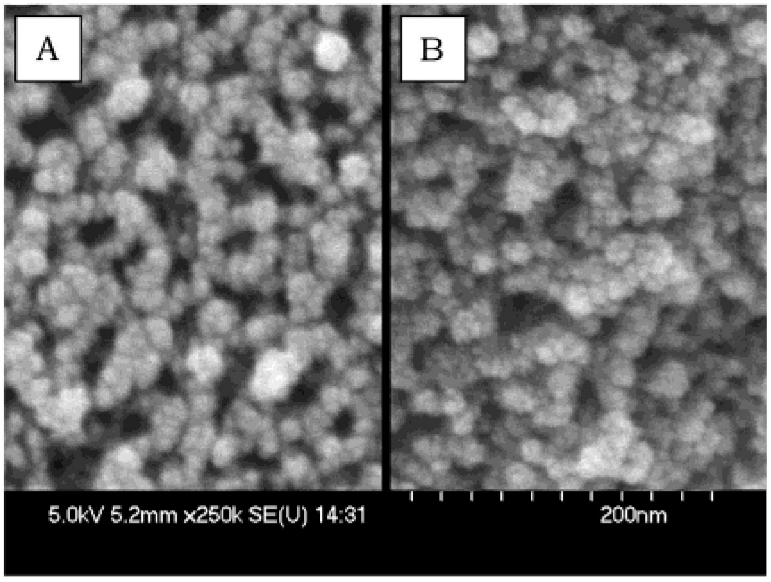

Figure 1.3a
SEM image of a native silica aerogel

Figure 1.3b
SEM image of a derivatized silica aerogel

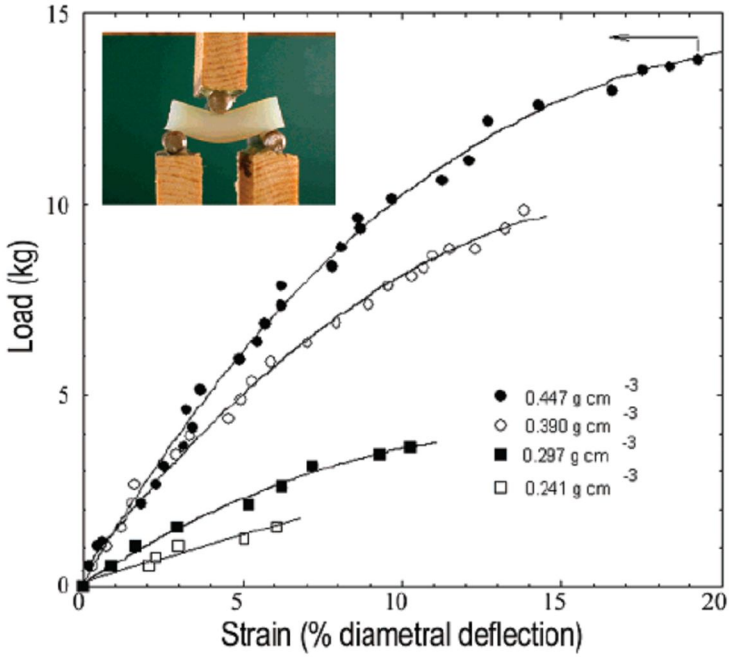

Figure 1.4
Mechanical properties with respect to density given by *Leventis et al*

Chapter 2: Experimental Section

2.1 Synthesis of Silica Aerogels

The synthesis of a native silica aerogel typically begins with the use of some form of silicon alkoxide such as tetramethyl orthosilicate (TMOS), which is shown in Figure 2.1, as your source of silica. When TMOS is in the presence of water it reacts with water which strips the TMOS of its organic group and replaces it with a hydroxyl group which bonds to the silicon. This process is called hydrolysis and these along with the condensation reaction are shown in Figure 2.2. Now, this newly formed hydroxyl group will then find other OH or OR groups and react to form a polymer while still suspended in a solvent (typically ethanol). This polymer chain is formed of siloxane bonds which then expand by either an alcohol-producing or water-producing condensation reaction.[4]

This causes all of these siloxanes to begin to form large groups which then begin to nucleate and grow together. This process is catalyzed by being in a basic environment. For this reason, in our reaction, native silica gels were synthesized using ammonium hydroxide. After the particles have completely aggregated, a solid monolith, or in this case a wet-gel, is formed which has the suspending solvent now filling its pores.[5] The next step for a native aerogel is to remove the solvent using supercritical drying. This topic will be discussed in more detail in Section 2.3.

Our synthesis method for silica aerogels differs in two ways. Firstly, all of our reactants are mixed during the gelling process. This one-pot synthesis is very desirable

for the improvement of applicability. This means we will often choose photoinitiators which are also basic so that they serve the dual purposes of catalyzing the gelation as well as providing radicals for the photopolymerization. Secondly, because our intention is to photopolymerize a monomer and have it conformally coat the sides of our silica gel, we need to make sure that our walls are derivatized by the desirable olefins.

As mentioned in Section 1.2, *Leventis et al.* had previously shown that they were capable of doing this and for this reason we also derivatized our walls using trimethoxysilylpropyl methylmethacrylate(MMA-TMOS) which is shown in Figure 2.3. This left us with a reactive group for our monomer to stick to that was also attached to the gel wall. So using a small concentration of MMA-TMOS in addition to our TMOS, we were able to, in a one-pot synthesis, create a derivatized silica aerogel which had bonding sites for our monomer.[6] As mentioned in the literature review, the ability to force our polymer to adhere to the surface of the gel creates a great deal more structural stability as well as allowing for lower monolith densities.

2.2 Laser Modification of Sol-gel

2.2.1 Ultraviolet System

Free radical polymerization is a method of polymerization by which a polymer forms by the successive addition of free radical building blocks. Photopolymerization using free radicals can be done using what is called a photoinitiator. In our case 2,2′-azobis-isobutyronitrile (AIBN), Figure 2.4, was used due

to it being highly soluble in the monomer and solvent as well as its high absorption of ultraviolet light. To go from monomer/initiator solutions to producing polymers by free radical polymerization, one must first begin initiation.

This step begins when an initiator decomposes into free radicals in the presence of monomers. In our system, due to the instability of carbon-carbon double bonds in the vinyl monomer, the unpaired electrons in the radical will readily react with our monomer to begin polymerization. In this reaction, the active center of the radical takes one of the electrons from the double bond of the vinyl monomer, leaving an unpaired electron to appear as a new active center at the end of the polymer chain. Addition of new monomers then readily occurs and our chain grows. This process is shown in Figure 2.5.[6]

Using this method, luminescent patterns were generated by exchanging the solvent of a gel with an acetonitrile solution containing 1% (w/w) of 9-vinylanthracene (Figure 2.6) and 0.1% (w/w) of AIBN. To create uniformly cross-linked monoliths samples were exposed to a commercial 15 W black light or to a 30 mW He-Cd laser (325 nm) expanded by a divergent lens. To create surface patterns, a 175 mW continuous wave (CW) laser (Coherent MBD-266) emitting at a wavelength of 266 nm was employed.

The 266 nm wavelength was strongly absorbed by both the matrix and the organics, resulting in patterns that did not penetrate more than a few millimeters. To create three dimensional patterns the third harmonic (354 nm) of a pulsed yttrium aluminum garnet (Nd:YAG) laser (EKSPLA 312 G) was employed. The pulse duration

was 150 ps and they were focused inside the bulk of the monolith by a lens with a focal length of 100 mm. The mean pulse energy was kept below about 10 mJ to prevent damaging the matrix. This was limited however by the strong absorption of both the initiator and the organic solvents used.[6] For this reason, a significant amount of the beam was absorbed before reaching the focal point of the laser. Detailed features were obtained with a size below about 30 μm. Exposure times were between 2 and 10 min when a laser was employed and up to 48 h for exposure with a black light ($\lambda \approx 370$ nm). After exposure, monoliths were washed repeatedly with toluene to remove unreacted precursors that were not readily attached to the walls. Afterwards, gels were washed with ethanol to prepare them for supercritical drying.

One of the major drawbacks of most conventional photoinitiators is that they are radicalized by ultraviolet (UV) light, which has several disadvantages for fabrication of anisotropic materials.[6] Short-wavelength UV light does not penetrate deeply within a monolith because of absorption of both the organics, but also the monolith itself. More importantly scattering from the polymer and from the oxide backbone prevents fabrication of well-defined patterns that reach deep into the bulk.

2.2.2 Visible System

Our system for free radical photopolymerization using visible light is very similar to that of our UV system, but with a few modifications to improve reactivity and significantly reduce scattering and undesirable absorption. These goals were accomplished by using a more reactive monomer, Hexanediol diacrylate, a radical polymerization catalyst, pentaerythritol tetra-(3-mercaptopropionate), and a new visible

light initiating system which are all shown in Figure 2.6-10. The coinitiators in our new system are a well-studied system which was described thoroughly by *Bowman et al.* in *The Journal of Polymer Science: Part A: Polymer Chemistry* in 2009. This new system uses a dye, Eosin Y, a tertiary amine as a coinitiator, N-methyldiethanolamine, and a monomer to initiate polymerization.

In the abovementioned paper, *Bowman et al.* describe how even in the presence of high concentrations of polymerization inhibitors (dissolved oxygen, radical scavengers, etc) polymerization was still able to be initiated using visible light. This new coinitiator system has the flexibility to be used with a wide variety of chemistries due to the robust efficiency of radical generation. This new flexibility coupled with our catalyst greatly increases the mobility and availability of radicals in exposed regions. This increase in the number of radicals is very favorable for our new monomer which unlike our UV monomer, has two vinyl bonds which can be radicalized and linked with other monomers.[10]

Because of the strong absorption of green light by our dye, samples were exposed to the green (532 nm) light of a diode-pumped solid state laser (Coherent Verdi) operated with a power of 1W. To achieve functionally graded materials, the beam was expanded through a lens so as to cover the diameter of the sample. The cylindrical samples were then exposed longitudinally so that power density would diminish as the beam width increased along the axis parallel to the beam exposure. Samples which were photocross-linked in only one specific region were obtained by exposing transversely to an expanded beam. Samples were rotated at half the exposure

time to ensure an even dose over the exposed region. To create grid patterns, a pinhole was placed between the sample and the laser beam. The sample was then moved by an X-Y programmable translation stage (NewportXPSC-8) along a predetermined path.[6,7] Exposure times were between 2 and 15min for the large-scale patterns; grids were obtained by scanning the sample in front of the beam with a velocity of 1 mm/s. After exposure, samples were washed in toluene to terminate polymerization as well as remove any unreacted monomer/initiator from the monolith.

2.3 Supercritical Drying of Silica Aerogels

After exposure, monoliths were washed repeatedly with excess amounts of ethanol to remove unreacted precursors that would create a pressure differential within the aerogel because of differing supercritical points. For drying, we employed a 2 liter Parr pressure vessel equipped with three external heaters supplying a maximum power of 800 W. The samples were placed inside the vessel and about 650 ml of excess ethanol were added to prevent complete evaporation of the solvent within the pores of the gels before the supercritical temperature was reached. The vessel was then heated to reach supercritical conditions for ethanol (240°C, 60.6 atm); left for about 30 min at the supercritical temperature and pressure and then the vaporous ethanol was then evacuated until no solvent remained in the vessel.[4]

As the substance in a liquid body crosses the boundary from liquid to gas, the liquid begins to gradually change to a gas, while the volume of the liquid shrinks. In a

heterogeneous environment, surface tension formed at the liquid/gas interface resists the change. Delicate structures, such as the pore structure of aerogel, tend to be broken apart by this surface tension at the liquid–solid interface.[4]

Supercritical drying goes around the line to the right, on the high-temperature, high-pressure side Figure 2.11. This route from liquid to gas does not require any phase change, but instead passes through the supercritical region, where the distinction between gas and liquid ceases to apply. Densities of the liquid phase and vapor phase become equal at the critical point of drying which creates a system where there is no surface tension between the fluid and the walls. Once venting begins (reducing pressure), the solvent is removed, and due to the temperature, the solvent goes into its gaseous form which does not create surface tension with the pore walls upon extraction. Once the solvent is completely removed, only the aerogel, with no solvent, remains. A schematic of the drying vessel is shown in Figure 2.12

Chapter 2 Figures

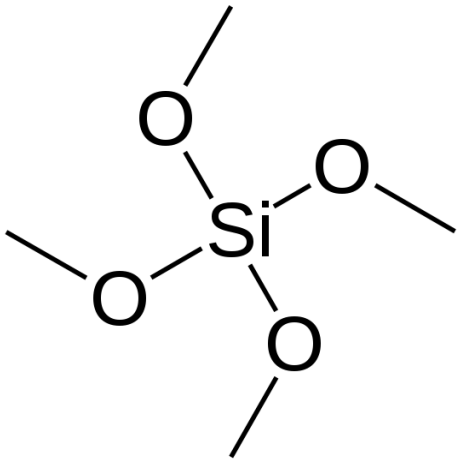

Figure 2.1 Tetramethylorthosilicate (TMOS)

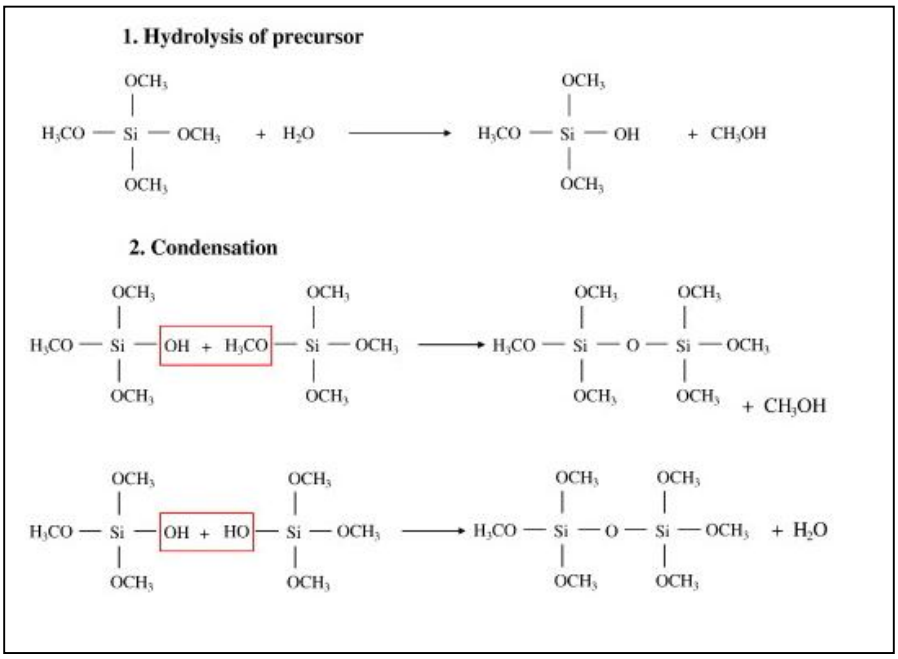

Figure 2.2
Hydrolysis and Condensation in Silica Aerogels

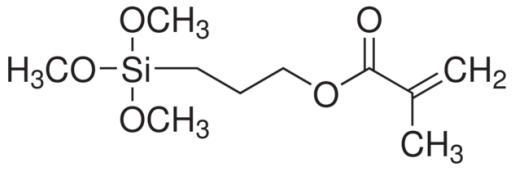

Figure 2.3
trimethoxysilylpropyl methylmethacrylate (MMA-TMOS)

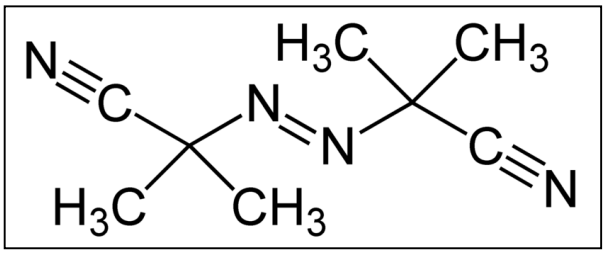

Figure 2.4
Azobisisobutyronitrile

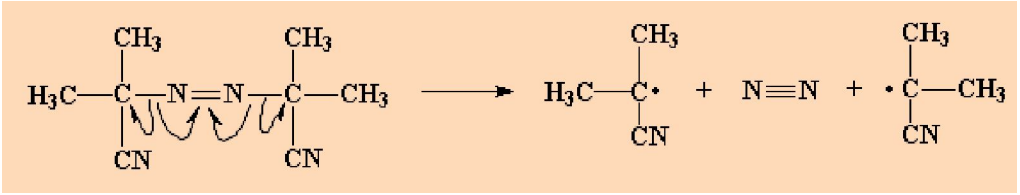

Figure 2.5
Photoinitiation of AIBN

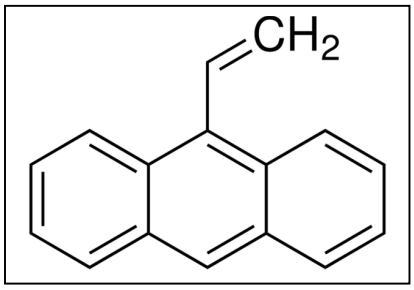

Figure 2.6
9-vinylanthracene

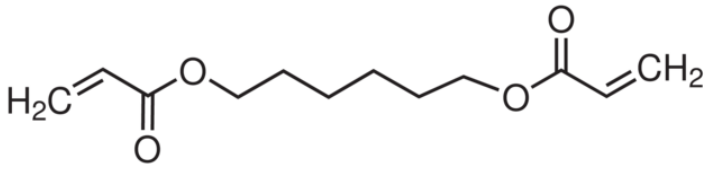

Figure 2.7
Hexanediol Diacrylate

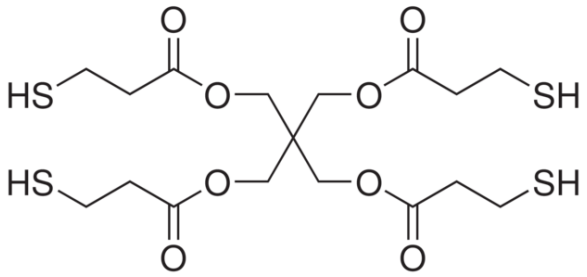

Figure 2.8
Pentaerythritol tetrakis(3-mercaptopropionate)

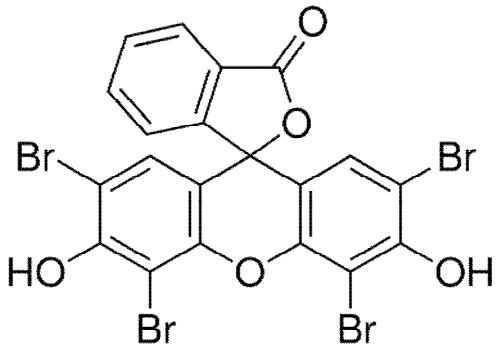

Figure 2.9
Eosin Y

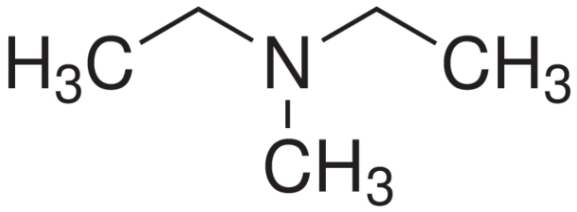

Figure 2.10
diethanolmethylamine

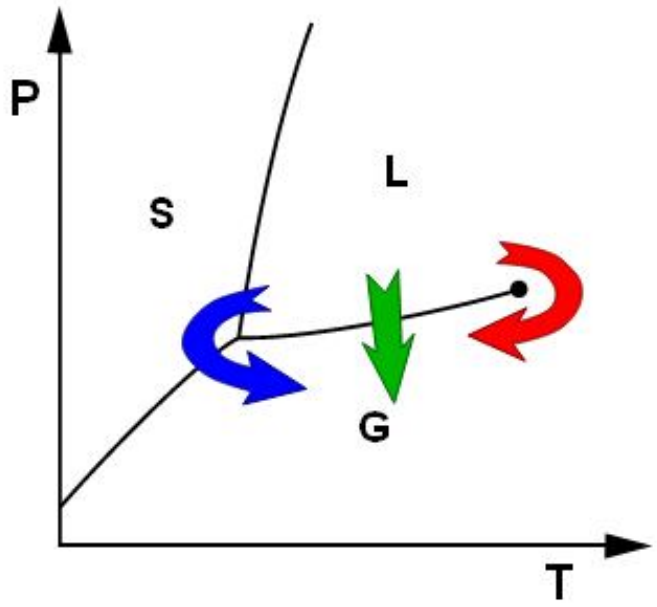

Figure 2.11
Possible phase changes
Red being Supercritical path

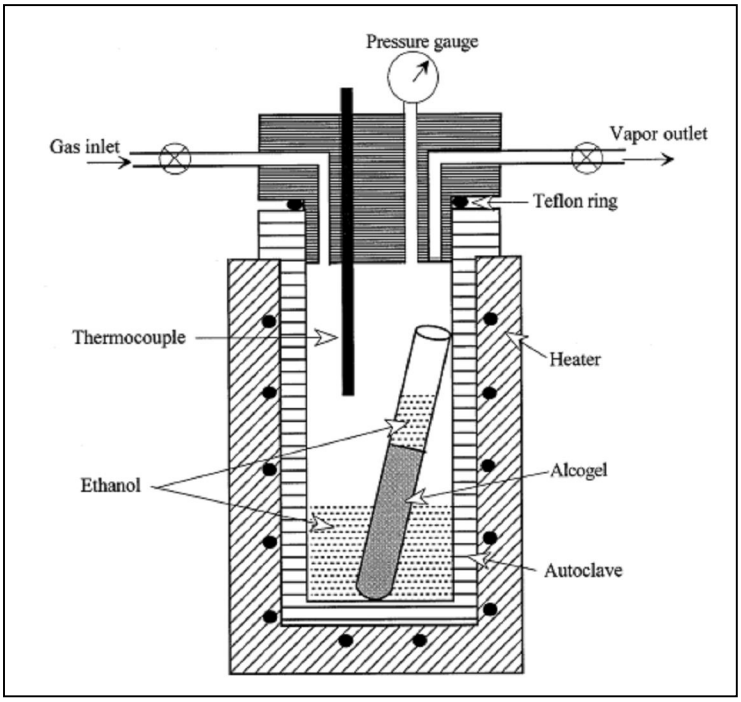

Figure 2.12
Schematic of a Supercritical Drier

Chapter 3: Results

3.1 SEM / AFM

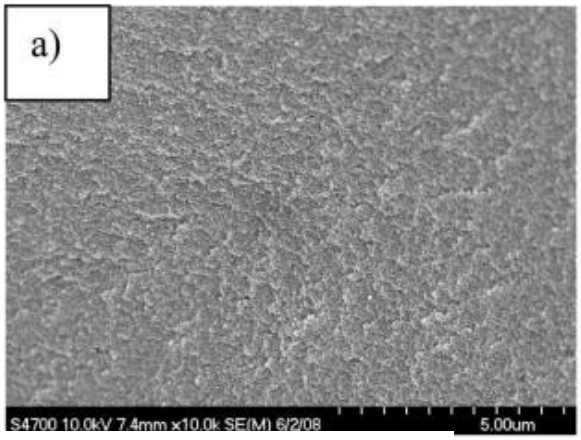

Figure 3.1a
Derivatized Silica Aerogel

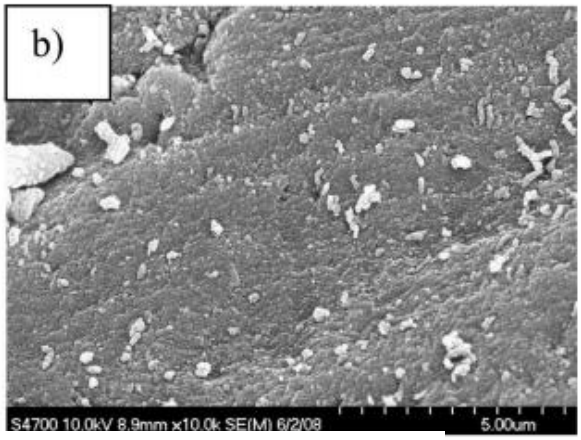

Figure 3.1b
Underivatized Silica Aerogel

Representative SEM images of monoliths supercritically dried in ethanol after photopolymerization are shown in Figure 3.1a. Due to the electrically insulating properties of silica aerogels, samples were sputtered with a thin layer of platinum to increase the electron generation. Low magnification images showed a relatively flat and homogeneous surface for the samples which were derivatized.[7]

This is highly indicative of a lack of aggregated polymer sitting on the surface of the aerogel. This runs contrary to our native gels which showed varying sized aggregates of polymer on littered all over the surface. This is consistent with the presence of large polystyrene particles which was confirmed by the optical analysis and

Raman analysis.[7] Optical analysis and Raman Spectroscopy results will be covered in greater depth in Section 3.3 and Section 3.4 respectively.

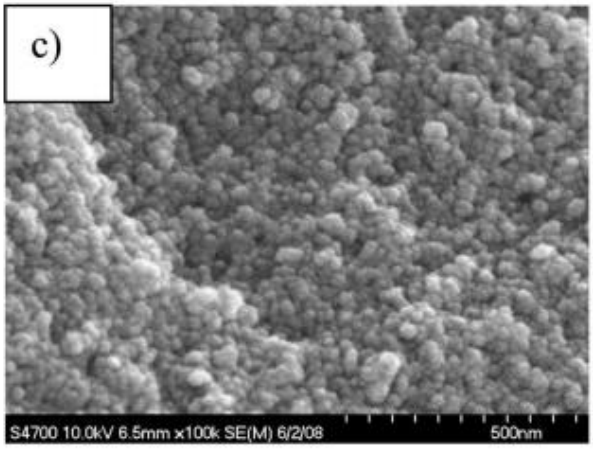

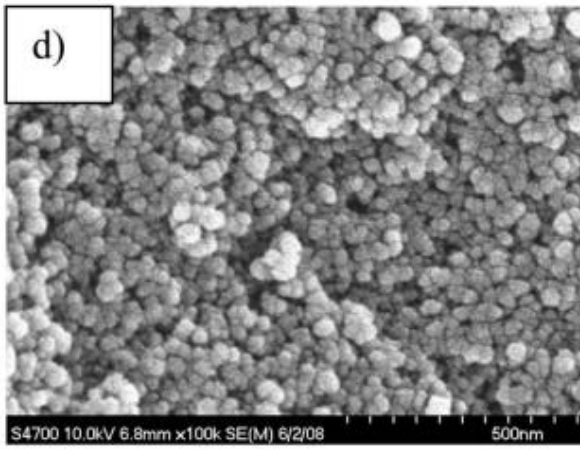

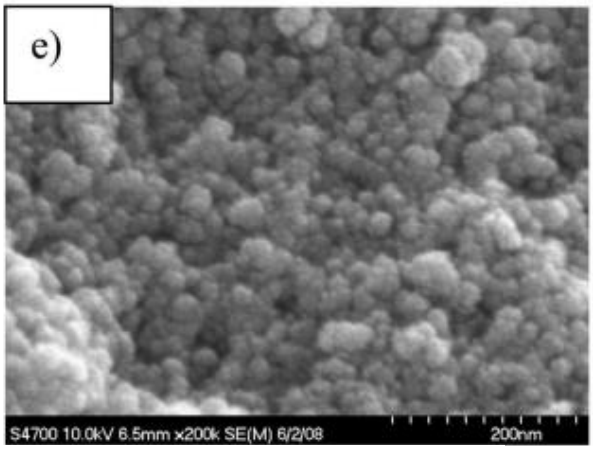

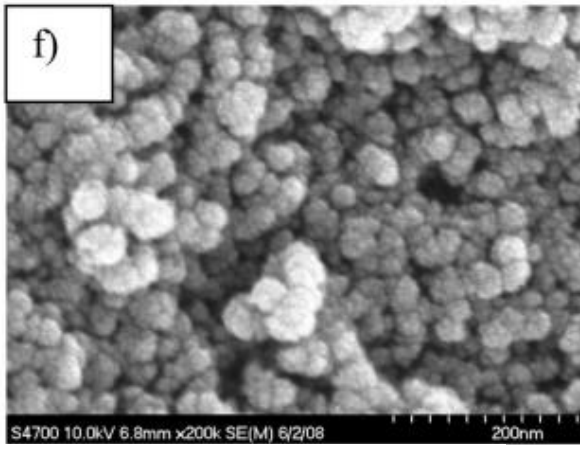

Figure 3.2c,e
Derivatized Silica Aerogel

Figure 3.2d,f
Underivatized Silica Aerogel

High magnification images showed further differences. In silica aerogels, primary silica particles with a diameter in the 2-10 nm range aggregate to form secondary agglomerations with a diameter in the 20-40 nm range. Primary and secondary aggregations were clearly visible in native gels, as shown in parts d and f of Figure 3. In

derivatized gels only the secondary aggregations were clearly visible (Figure 3c,e). Overall, the SEM results are consistent with those obtained from samples cross-linked by thermally activated polymerization and indicate that a network of cross-linked silica nanoparticles is formed by photo-crosslinking.

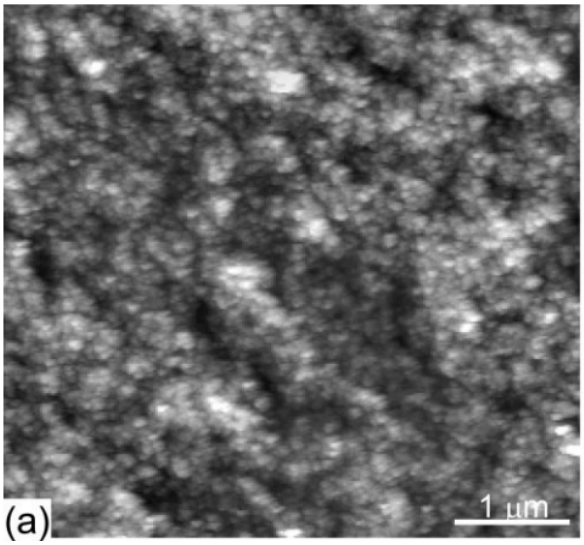

Figure 3.4a
Derivatized Silica Aerogel

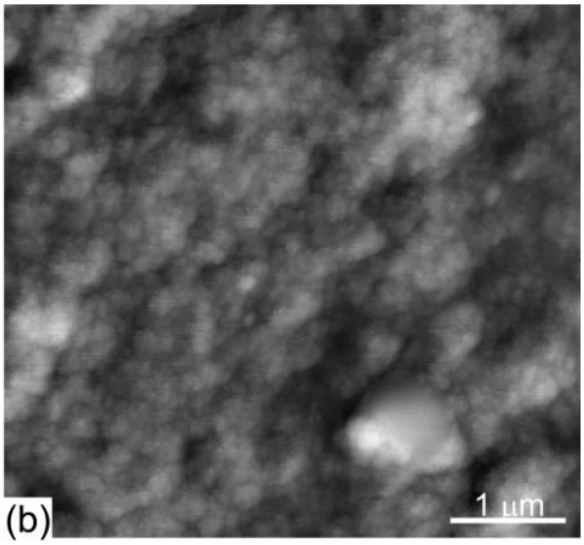

Figure 3.4b
Underivatized Silica Aerogel

The SEM results were further supported by AFM. Because of the low density of aerogels, the AFM tip tended to lift the samples generating high noise levels. Therefore, xerogels were employed. Figure 3.3a shows the typical morphology of a derivatized sample before photopolymerization. Granular aggregates with a size of tens of nanometers could be resolved, which likely corresponded to the secondary aggregations.[6] After polymerization the size of these aggregations increased (Figure 3.3b).[7]

3.2 FT-IR / Raman Spectroscopy

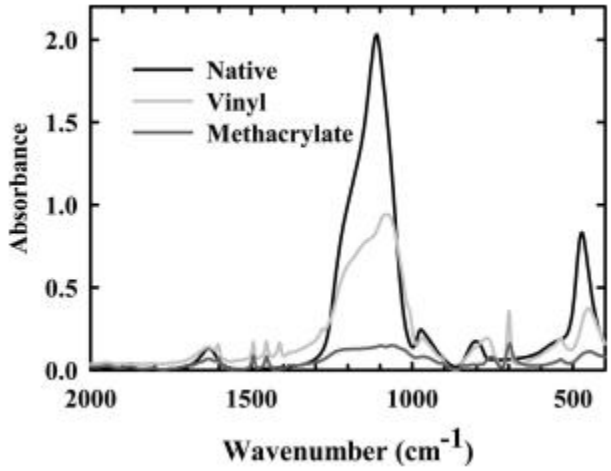

Figure 3.5
FT-IR Spectrum

FT-IR spectroscopy measurements are shown in Figure 3.5 and provide some insight on the parameters affecting the cross-linking process. Native aerogels exhibited broad and intense bands below 1300 cm^{-1} which are characteristic of silica. The most intense of these bands was in the 1100-1200 cm^{-1} range and was attributed to Si-O stretching. In photopolymerized samples (both native and derivatized) we also detected a broad band around 1620 cm^{-1} which was attributed to modes of the aromatic ring of polystyrene.[11] In samples derivatized with vinyl and methacrylate, additional small and narrow bands were detected which most likely were due to the derivatizing moiety.

These were at 696 cm^{-1}, which is close to the range of CH_2 rocking; at 1409, 1449, and 1493 cm^{-1}, which are within the range of C-H bending; and at 1603 cm^{-1}, which is within the range of CdC stretching. We also noticed that the intensity of the

silica bands decreased in derivatized samples. The decrease in the intensity of the silica vibrations is similar to that observed in oxide-polymer core-shell nanoparticles, and it is a further indication that in derivatized samples the pore walls are coated with the polymer.

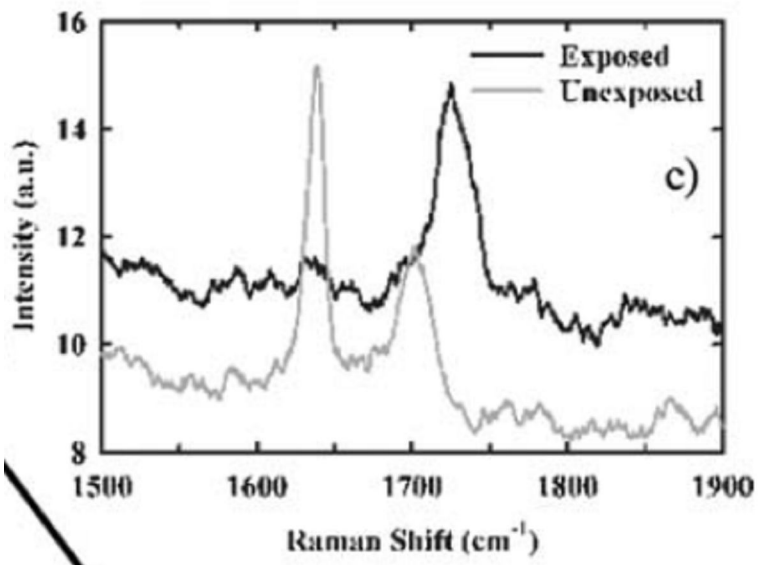

Figure 3.6
Raman Spectrum of Exposed Silica Aerogel

In Figure 3.6, Raman Spectroscopy measurements are presented which further corroborate our findings. The strong peak at 1636cm^{-1} is from the Carbon-Carbon double bond. The sharp drop of between exposed and unexposed regions is a strong indicator of allyl polymerization and in conjunction with FT-IR gives a good idea of the elemental makeup of our differing regions.

3.3 Images

3.3.1 UV System

The below images were taken using a digital camera. They all represent images taken using 9-vinylanthracene as the monomer. The 9-vinylanthracene can be shown fluorescing under black light illumination. In Figure 3.7, one can see that the pattern was readily transferred from USAF mask to the aerogel. The yellow coloration is the unwashed 9-vinylanthracene which is fluorescing in the background.

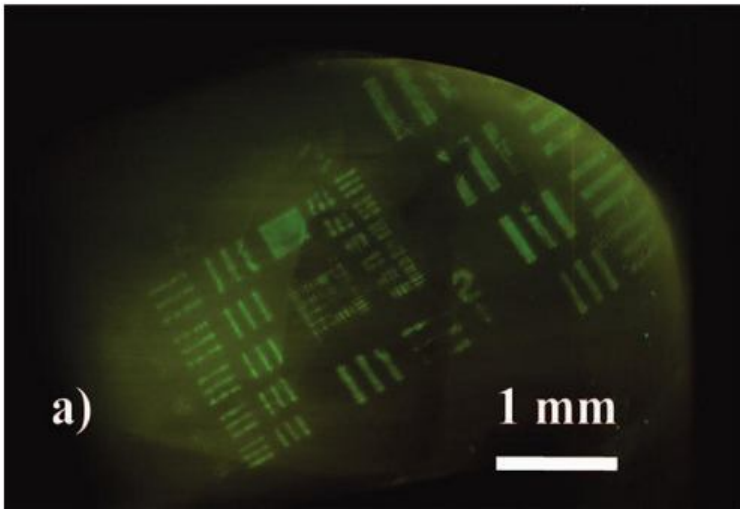

Figure 3.7
Gel Exposed using the UV System a 1951 USAF resolution test mask.

As mentioned above, pulse laser lithography was also employed with the UV system to attempt to make deeper penetrating, high resolution patterns. Because the 266nm wavelength laser did not penetrate into the gel due to absorption, the third harmonic of the Nd:YAG laser was used. The 355nm wavelength allowed for better

penetration depth, but due to scattering and some absorption by solvents as well as the initiator/monomer, the resolution and depth were reduced. Below in Figure 3.8, an image can be seen with a pulse laser treated sample. Due to fluorescence by the solvent, the gel glows blue. The white, vertical running line is polyvinylanthracene.

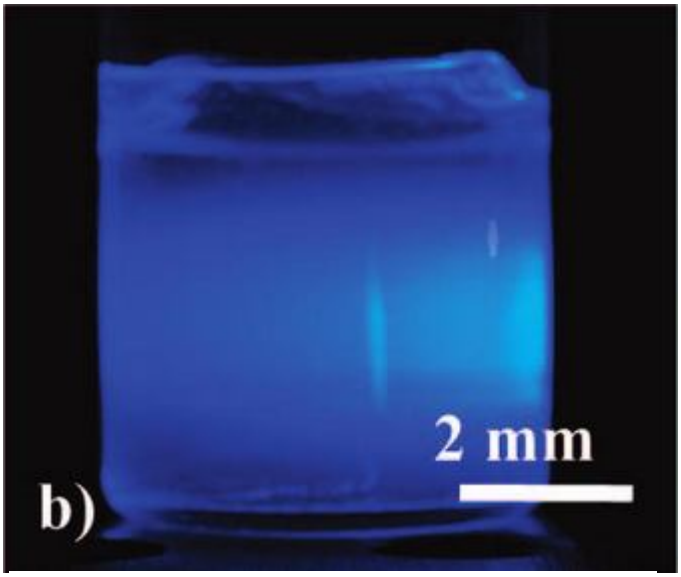

Figure 3.8
Gel exposed using the UV System (λ ≈ 355nm) and 9-Vinylanthracene. Sample was focuses through a 100mm focal length lens.

Below is an example of a native aerogel(3.9a) and a native, polymer-saturated sample(3.9b). The polymer saturated sample did not have a derivatized surface. Because there were no binding sites for the polymer on the silica matrix, polymer grew and simply clogged the pores. This is an example of what previous works had attempted to do with polymer reinforcement before Leventis et al. The white coloration comes from the large abundance of polymer which fills the pores of the aerogel.

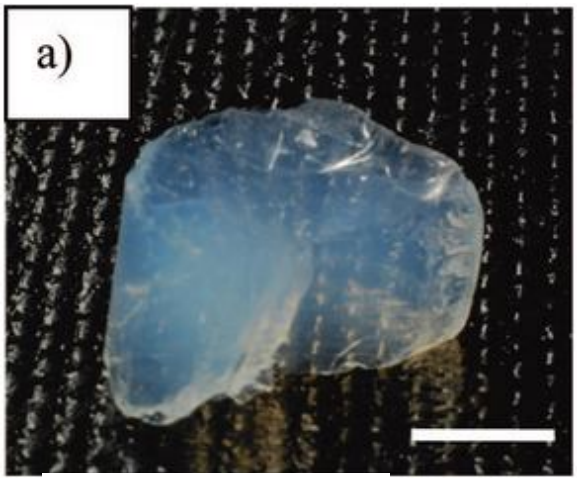

Figure 3.9a
Native Silica Aerogel

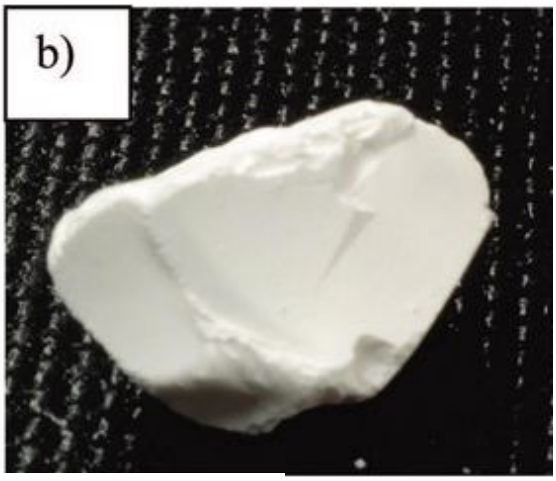

Figure 3.9b
Polymer Saturated
Native Silica Aerogel

Figure 3.10, an image of a functionally graded aerogel is presented where its cross-linked region is glued to a glass slide with cyanoacrylate adhesive. Shearing of the glued region from the rest of the aerogel was not observed, as is instead, commonplace for native aerogels.

Presented in Figure 3.11, a bolt was threaded into a hole which was drilled and tapped for a 2–64 thread inside a polymer reinforced region of aerogel. The structural support provided by the polymer backbone allows for local forces to be dampened and not collapse or shear the gel structure.

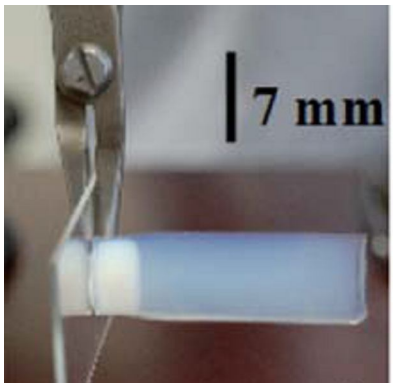

Figure 3.10
Visible Patterned Silica Aerogel fastened to a glass slide.

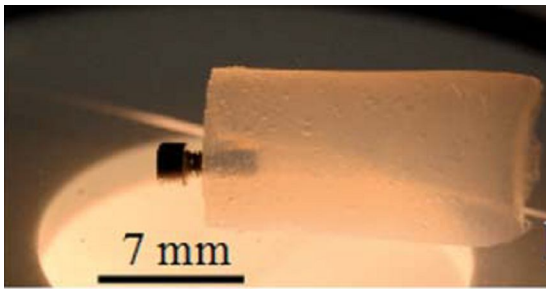

Figure 3.11
Reinforced Aerogels are mechanically strong enough to be drilled, tapped, and threaded with small bolts.

In Figure 3.12 one of the photopolymerized gels is presented which has been moved on the X-Y stage. The pattern can be placed with speeds ~1mm/s and penetrates well beyond 25 mm with only a very limited amount of spreading or loss of resolution. Polymer growth/shrinkage can frustrate attempts at small details, but by adjusting dye concentration, speed, and laser power, one can compensate for the projected polymer size fluctuations.

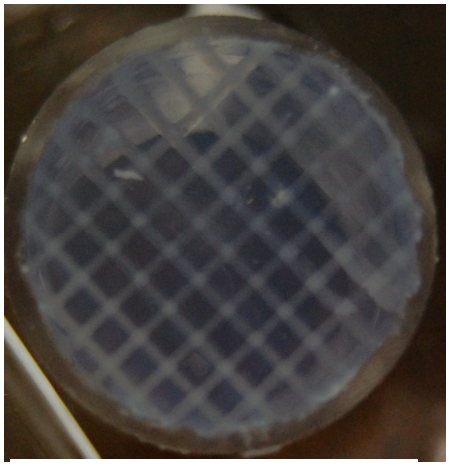

Figure 3.12
Patterned Aerogel

The below image (Figure 3.13) contains a test which used contact angles to measure the hydrophobicity of the sample. Because the polymer and surface functional group are both hydrophobic where as native aerogel tends to be hydrophilic, one can see determine the amount of polymer present along a gradient on ones sample by simply seeing the angle between the water droplet and the aerogel surface.

If you notice, the polymer gradient can clearly be seen in the image as the white haze. As one moves to the right, the gradient diminishes to very little polymer present. At the very far left, the water beads very tight. This indicates strong hydrophobicity. If one looks at the very far right, the bead can be seen almost completely flat. This indicates a strong hydrophilicity. As one follows the length of the sample, one can see that the contact angle of the water beads, becomes smaller and smaller as it you move towards the right. This is very clear proof that a polymer gradient has been formed during exposure.

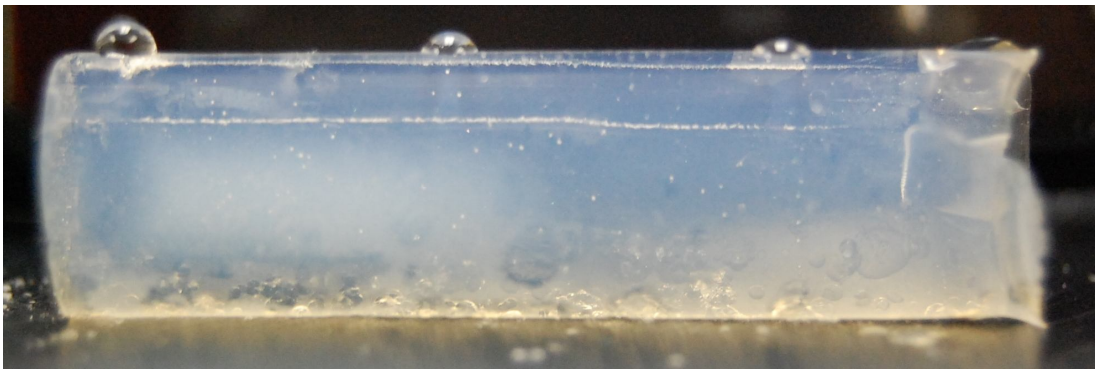

Figure 3.13
Test for functionalization of hydrophobicity. Polymer side is visible on the left and is the most hydrophobic due to hydrophobic polymer cross-linked onto the derivatized pore Figure 3.13

Chapter 4: Conclusions

4.1 UV System

In the above work, a method has been shown that allows for bulk sol-gel monoliths with spatially modulated physical properties to be produced by photocrosslinking. Topical exposures as well as better penetrating methods have been shown and obtained by using suitable light sources and illumination conditions. This method is simple and extremely versatile because it combines the flexibility of sol-gel and polymer chemistry. While some limiting factors still remain when using ultraviolet lithography inside of silica, this was more a proof of concept and there is still a large degree of freedom available to make this system worth pursuing further in the future.

With this system, multifunctional sol-gel monoliths can now be realized which have potential applications in microfluidics, optics, mechanics, and acoustics where the physical properties of aerogel are strongly desirable, but require some slight alteration of the properties. Due to the wide array of polymer chemistry available with this technique, one could very easily tune the properties of the aerogel to within acceptable tolerances.

4.2 Visible Light System

Similar to the ultraviolet system, photopolymerization with visible light allows fabrication of anisotropic aerogels and ceramic materials. However, due to the

transparency of silica aerogels to the visible spectrum, the tuneability of the dye/amine coinitiator system, and the reduced scattering of visible light, materials with very different characteristics can be produced by simple variations of the illumination and/or processing conditions without a great deal of difficulty or cost.

The above materials represent a new class of porous anisotropic solids that are difficult to fabricate with conventional polymerization/reinforcement methods and pave the way for several practical applications. For instance, functionally graded aerogels are likely candidates for ultra-lightweight energy absorbers. Selective reinforcement of regions subject to shear and mechanical stress allows integration of native aerogels into mechanical systems. Honeycomb patterns increase the compressive strength of an aerogel along the load-bearing direction while the monolith retains the porous structure of the native material for minimum thermal conductivity and maximum acoustic attenuation.

The problem of the need for supercritical drying still hamstrings the adoption of silica aerogels for industrial adoption, but the shortcomings of the isotropic methods shown earlier have for the most part been minimized if not removed altogether. Work will need to continue to tailor aerogels to meet current industrial standards and tolerances, but with the systems presented here, several major issues have been resolved without adding any considerable cost to the processing.

References

(1) Hench, L. L.; West, J. K. *Chem. Re*V. **1990**, *90*, 33-72.

(2) Husing, N.; Schubert, U. *Angew. Chem., Int. Ed. Engl.* **1998**, *37*, 22-45.

(3) Fricke, J. *Sci. Am.* **1988** (March), 92-97.

(4) Pierre, A. C.; Pajonk, G. *M. Chem. ReV.* **2002**, *102*, 4243

(5) Leventis, N.; Sotiriou-Leventis, C.; Zhang, G.; Rawashdeh, A.-M. M. *Nano Lett.* **2002**, *2*, 957.

(6) C. Wingfield, A. Baski, M. F. Bertino, N. Leventis, D. P. Mohite and H. Lu, *Chem. Mater.*, **2009**, 21, 2108.

(7) Charles. Wingfield , Louis. Franzel , Massimo. F. Bertino and Nicholas. Leventis *J. Mater. Chem.*, **2011**, 21, 11737-11741

(8) Nemeth, S.; Yin, R.; Ottenbrite, R. M.; Siddiqui, J. A. *Polym. Prepr.* **1997**, *38*, 365-366.

(9) Chiang, T. H.; Nakamura, A.; Toda, F. *Thin Solid Films* **1989**, *182*, L13-L16.

(10) H. J. Avens and C. N. Bowman, J. of Polymer Sci., 2009, 47, 6083.

(11) Ilhan, U. F.; Fabrizio, E. F.; McCorkle, L.; Scheiman, D.; Dass, A.; Palzer, A.; Meador, M. A. B.; Leventis, N. *J. Mater. Chem.* **2006**, *16*, 3046.

(12) Gatic, N.; Fernandez, N.; Opazo, A.; Alegria, S.; Gargallo, L.; Radic, D. *Polym. Int.* **2003**, *52*, 1280

(13) D. Burget, C. Mallein and J. P. Fouassier, Polymer, **2004**, 45, 6561.

(14) P.-W. Wu, W. Cheng, I. B. Martini, B. Dunn, B. J. Schwartz and E. Yablonovitch, Adv. Mater., **2000**, 12, 1438.